EXECUTIVE SUMMARY

In Situ Sequestration of PFAS from Contaminated Groundwater using Injectable High Affinity Cationic Hydrophobic Polymers

Jon Chorover
Leif Abrell
Jim Field
Reyes Sierra-Alvarez
Neeraja Setlur
Anton Gomeniuc
James Hatton
Robert Root
University of Arizona

James Hatton
Jacobs

August 2024

SERDP Project ER22-3155

EXECUTIVE SUMMARY

Project: ER22-3155

TABLE OF CONTENTS

Page

LIST OF FIGURES

Page

LIST OF TABLES

Page

ACRONYMS AND ABBREVIATIONS

ADEQ	Arizona Department of Environmental Quality
DoD	Department of Defense
IEP	isoelectric point
PANI	polyanilines
PFAS	per- and polyfluoroalkyl substances
PFOA	perfluorooctanoic acid
PFOS	perfluorooctanesulfonic acid
POT	poly-*o*-toluidine
PV	photovoltaic
SERDP	Strategic Environmental Research and Development Program

1.0 INTRODUCTION

Per- and polyfluoroalkyl substances (PFAS) such as perfluorooctanoic acid (PFOA) and perfluorooctanesulfonic acid (PFOS), as well as a wide range of shorter and longer chain analogues, are persistent pollutants present in the subsurface at many Department of Defense (DoD) facilities due to the past use of fire-fighting foams. Because of their mobility and recalcitrance, these compounds can form long, dilute plumes that require allocation of substantial resources in their cleanup. At present, remediation of PFAS is limited to pumping the groundwater and ex situ treatment by adsorption, or in situ treatment by commercially available activated carbon (McGregor 2018, McGregor 2020) and an experimental combination of water treatment polymers and activated carbon (Simcik et al. 2019, Liu et al. 2020). Particles are difficult to inject into an aquifer because they can be either filtered by well materials (if used) and by aquifer sediments, concentrating amendments in the vicinity of the boring, or mobilized in aquifer solutions as a result of poor retention on geo-media surfaces. Injection by aquifer fracturing to avoid filtration and improve dispersion can result in uneven distribution of treatment materials. In addition, activated carbon removes some PFAS species (e.g., PFOS) quite well, but it is less effective at removing PFOA and shorter-length PFAS analogues, leading to uneven sequestration of chemicals of concern. These issues can potentially be addressed by employing high-affinity colloidal sorbents engineered to achieve long-lasting and selective PFAS sequestration, such as those developed under the previous project (ER18-1052, Sierra-Alvarez et al. 2019). The goal of this proof-of-concept study is to determine the feasibility of utilizing these high affinity sorptive polymers for injection into highly-productive sand and gravel aquifers for the in situ sequestration of PFAS from impacted groundwater at environmentally relevant concentrations.

2.0 OBJECTIVES

a. **Task 1. Assess surface chemistry and colloidal stability of polymers as a function of aqueous geochemistry.** *Hypothesis 1: Colloidal stability and hydrodynamic diameter of polymer particles depend on a functional relation between polymer surface charge and aqueous chemistry.*

b. **Task 2. Measure retention of polymer in saturated sand.** *Hypothesis 2: The breakthrough curve behavior of polymers in a given saturated sand matrix is a function of (i) geomedia surface chemistry, (ii) polymer colloid properties (studied under Task 1), and (iii) aqueous geochemical conditions.*

c. **Task 3. Quantify the adsorption-desorption behavior of PFAS in polymer-sand matrices**. *Hypothesis 3: Adsorptive affinity will be similar for adhered and non-adhered polymers (the latter measured in the current study), but adsorption capacity will be modestly reduced as a result of consumption of polymer interfacial area in the grain adhesion process.*

d. **Task 4. Test PFAS adsorption for an impacted groundwater sample and quantify uptake of 25 recommended PFAS compounds.** *Hypothesis 4: Flow of PFAS-impacted groundwater through geomedia comprising polymer-sand complexes will reduce dissolved PFAS concentrations to target remedial levels.*

3.0 TECHNICAL APPROACH

a. Polymer surface charge measurements were based on electrophoretic mobility while hydrodynamic diameter and aggregation rate measurements were made using dynamic light scattering. Scanning electron microscopy was used to confirm polymer morphology.

b. A predictive understanding of the transport and deposition (physicochemical filtration) of injectable high-PFAS-affinity polymer colloids in saturated geomedia is essential for predicting the fate and long-term effectiveness of these colloids once they are injected into groundwater aquifer systems. The transport of colloids from pore fluids to the surface of mineral grains is the result of interception, gravitational sedimentation, and Brownian diffusion (Tufenkji and Elimelech 2004). Rapid scale column tests were performed under saturated conditions with polymer infusions of varying geomedia surface chemistry, pH, and polymer suspension concentration.

c. Single point adsorption batch experiments were performed at pH 6 to quantify and compare polymer adsorption capacity at equilibrium. Then, rapid scale saturated column experiments were performed, also at pH 6, to quantify polymer adsorption capacity as part of the polymer-sand matrix in a flow-through regime.

d. Groundwater samples from Former Naval Air Station Joint Reserve Base (NASJRB) Willow Grove (Site 5 and Hangar B 680) and a well operated by Tucson Water (production well C007A) were infused into columns pre-loaded with polymer for testing of PFAS removal in a flow-through system.

4.0 RESULTS AND DISCUSSION

Measurements of zeta potential for colloidal polyanilines (cPANI) (Figure ES-1a) and colloidal poly-*o*-toluidine (cPOT) (Figure ES-3a) show a circum-neutral isoelectric point (IEP) of cPANI (pH 6.76) and an acidic IEP for cPOT at pH 4.85. The hydrodynamic diameter measurements of cPANI increased with increasing pH with the smallest diameter observed at pH 4 (Figure ES-1b). Hydrodynamic diameter measurements for cPOT have high standard deviations for each measurement and all are above 2 µm (Figure ES-3b).

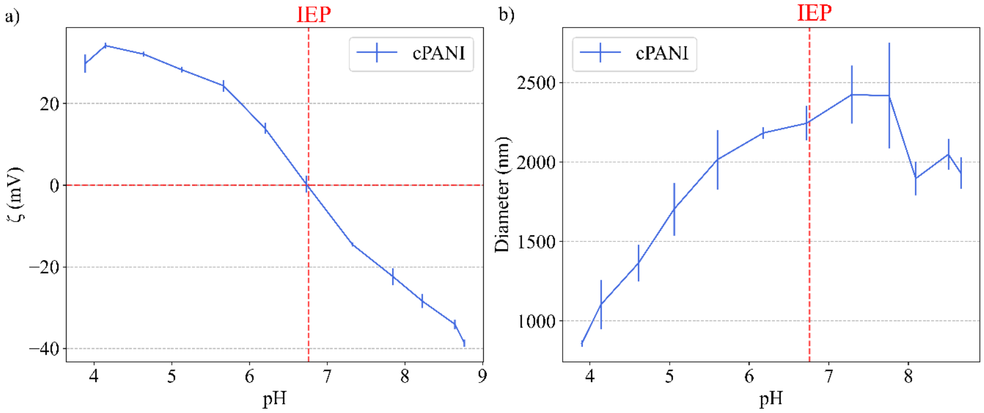

Figure ES-1. Dynamic Light Scattering Data for a) Zeta Potential and b) Hydrodynamic Diameter of cPANI as a Function of pH.

The pH at which the zeta potential equals 0 is the isoelectric point (IEP= 6.76).

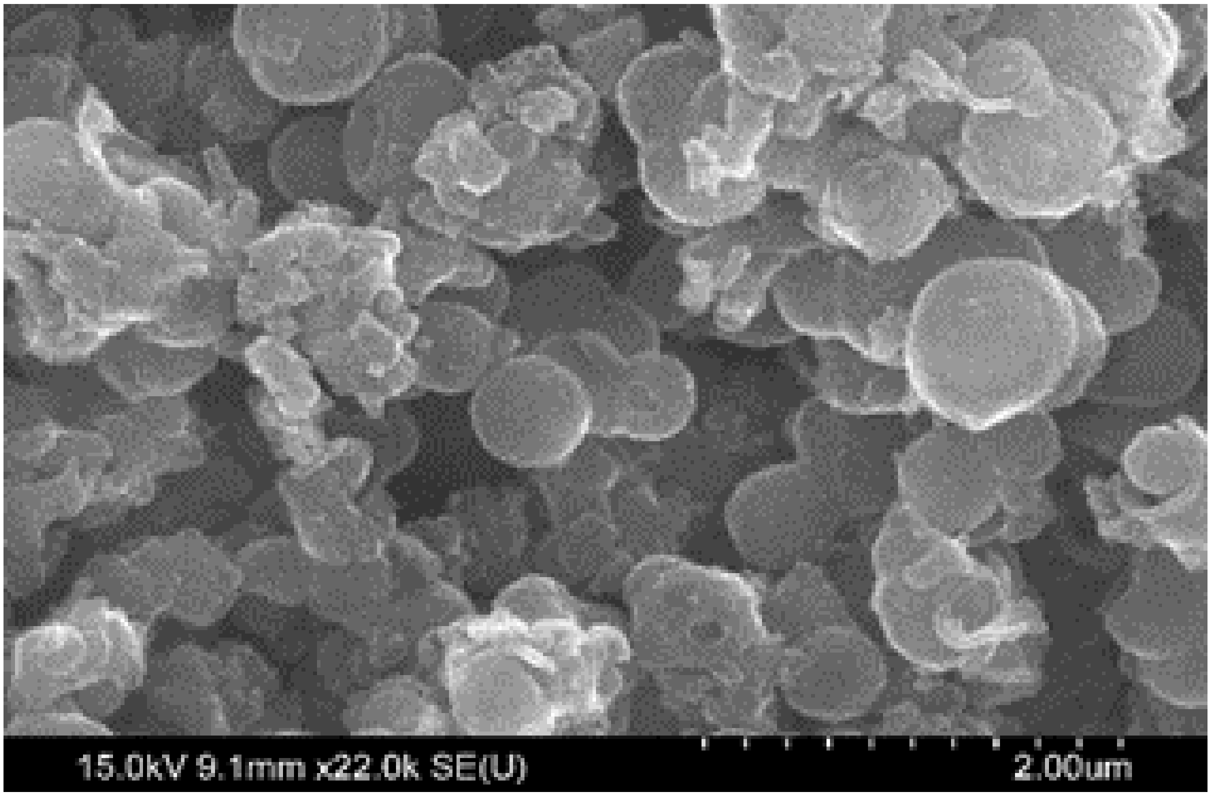

Figure ES-2. Scanning Electron Microscopy Micrograph of cPANI Showing Particles Are Sub-micrometer Spheres.

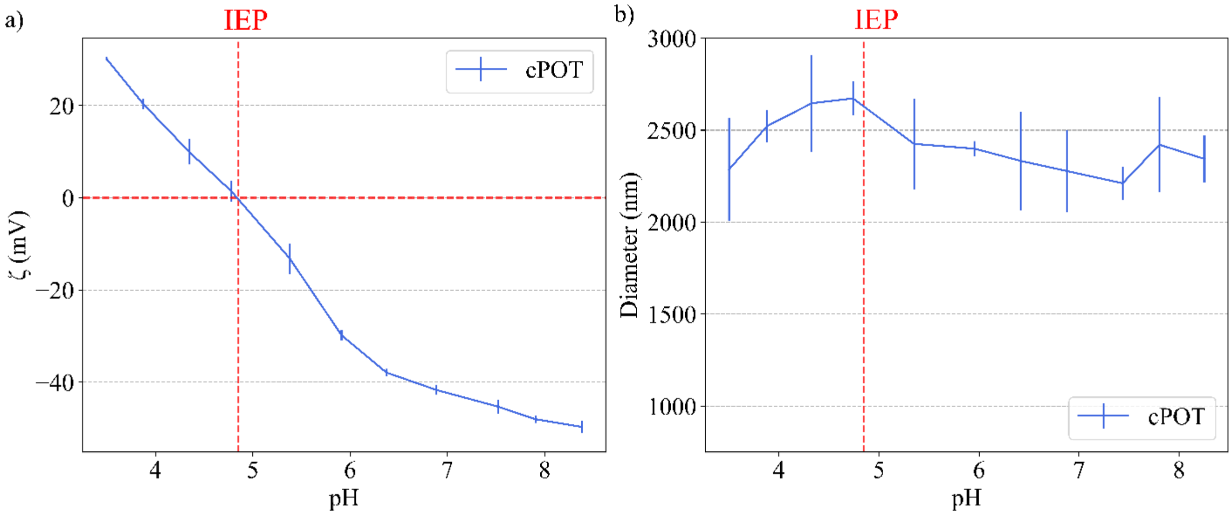

Figure ES-3. Dynamic Light Scattering Data for a) Zeta Potential and b) Hydrodynamic Diameter of cPOT as a Function of pH. The IEP is at 4.85.

In a single point batch experiment run at pH 6 with concentrations of 10 mg L^{-1} of polymer and 1000 ng L^{-1} of PFOA, cPANI exhibited an equilibrium sorbed mass (Q_e) of 98.34 ± 0.62 ng PFOA mg polymer-^{1}, a K_d of 4.11± 0.79 L mg^{-1}, and a removal efficiency of 97.59 ± 0.42 %.

When infused into columns at a suspension concentration of 10 mg L^{-1} in a 1 mM NaCl background electrolyte solution, the average loading of the cPANI was relatively high on both negatively and positively charged sand surfaces (Figure ES-4).

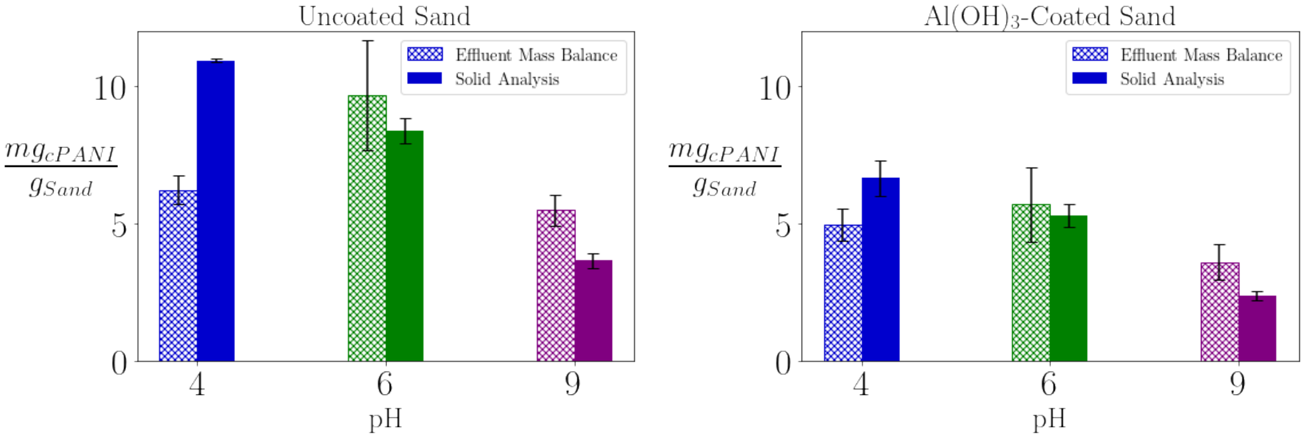

Figure ES-4. Average cPANI Loading Calculated from Column Experiment Effluent Mass Balance and Solid Dissection.

The black lines represent the standard deviation of duplicate samples.

The trends with pH and sand type seen in the results of this experiment were consistent with electrostatic interaction between the charged cPANI and the charged matrices. As shown in Figure ES-1a and discussed in previous sections, the IEP of cPANI was *ca*. pH 6, at which pH rapid aggregation occured. The higher particle aggregation may explain why the maximum loading was observed at pH 6, since cPANI-cPANI adhesion may be enhanced at this pH value. Al hydroxide coating of the sand increased cPANI charge repulsion by the surface, resulting in decreased retention, particularly at pH 4.

After infusing columns with a cPANI suspensions, the average cPANI loadings of the columns were 21.63 ± 5.02, 16.62 ± 5.02 and 18.25 ± 4.61 mg g^{-1} for Groups 1, 2, and 3 respectively. Each group of columns was then infused with 1 µg L^{-1} each of the eight representative PFAS species and, after around 6,500 photovoltaic (PV), 10x the original PFAS concentration. The columns showed a reduction by 90% for the majority of the PFAS over thousands of PVs at pH 6 (Figure ES-5).

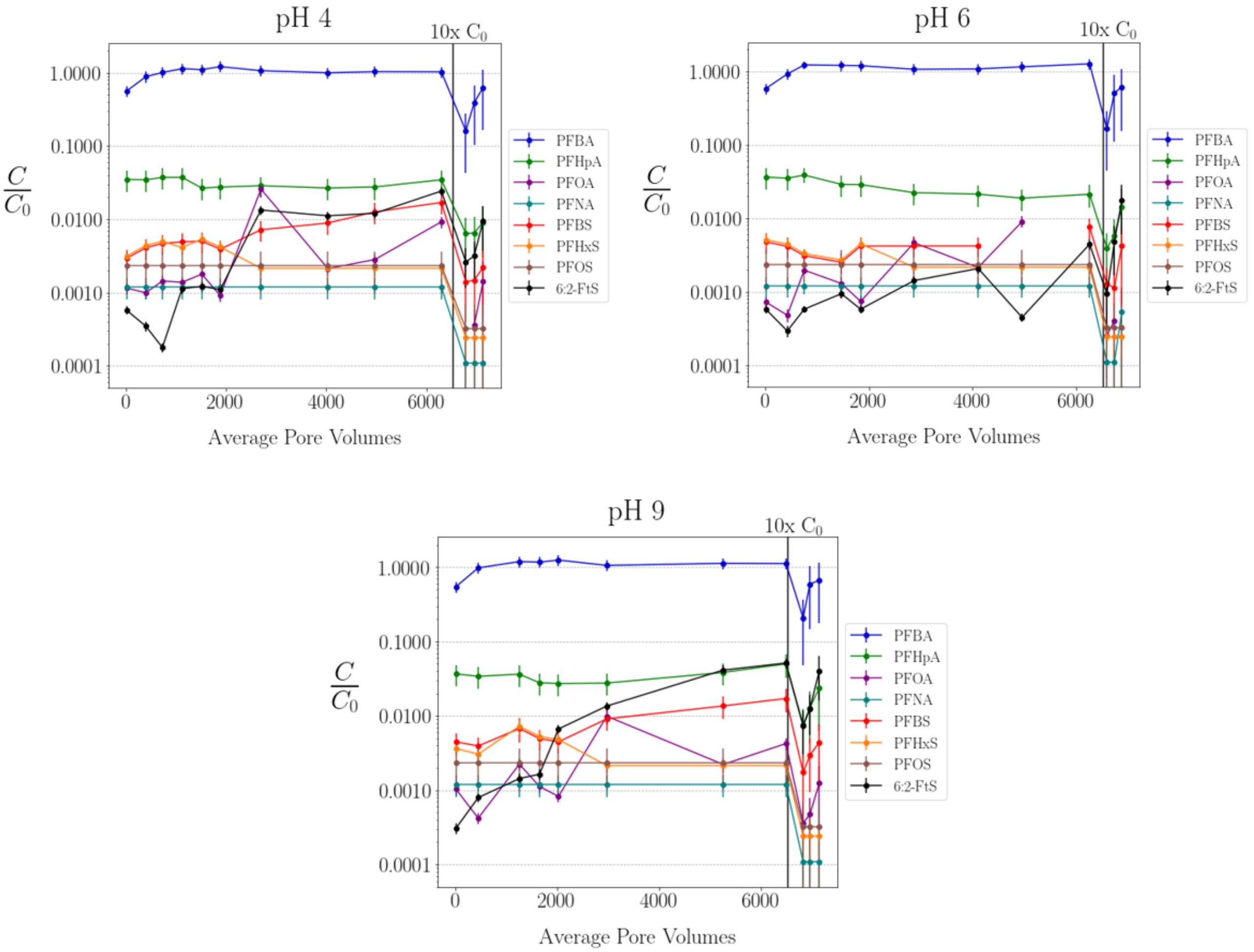

Figure ES-5. PFAS Breakthrough Following Infusion into the a) Group 1, b) Group 2, and c) Group 3 Columns from Experiment 1A.

The error bars at each point represent the standard deviation of triplicate samples. The vertical line labeled "10x C_0" represents the pore volume when the columns were infused with influent spiked to ten times the original concentration at time zero (shifted from 8 ng L^{-1} to 80 ng L^{-1} of total PFAS).

The performance of cPANI was then tested with three different groundwaters with a loading of 20 $mg_{cPANI}\ g_{Sand}^{-1}$. The pertinent chemical compositions of the groundwater measured by a DoD certified lab are included in Table ES-1.

Table ES-1. Chemical Composition of PFAS Impacted Groundwater Tested

(mean ± standard deviation shown).

	Willow Grove		ADEQ		
	Site 5 composite	**Hanger B composite**	**C007A composite**	**Units**	**LOD**
Measured TOF	5.6 ± 0.21	42.4 ± 0.04	12.500 ± 0.003	ug L^{-1}	5.1
Calculated TOF	3.6 ± 0.1	13.83 ± 0.04	6.66 ± 0.13	ug L^{-1}	
Analyte					
PFBA	500 ± 12	1700 ± 127	2260 ± 77	ng L^{-1}	97.5
PFHpA	102 ± 2	300 ± 28	210 ± 17	ng L^{-1}	2.5
PFOA	3300 ± 65	2300 ± 290	638 ± 9.3	ng L^{-1}	2.5
6:2 FTS	50 ± 1.7	3200 ± 110	2200 ± 100	ng L^{-1}	2.5
PFBS	80 ± 10	1109 ± 116.2	186 ± 1	ng L^{-1}	5.0
PFHxS	600 ± 200	5400 ± 620	1300 ± 110	ng L^{-1}	99.7
PFNA	18 ± 1.1	31 ± 2.9	2.7 ± 0.2	ng L^{-1}	5.1
PFOS	250 ± 5	4010 ± 50	1850 ± 38	ng L^{-1}	2.5
PFPeA	138 ± 9.1	680 ± 14	540 ± 22	ng L^{-1}	7.6
PFHxA	199 ± 8.4	1480 ± 14	760 ± 26	ng L^{-1}	2.5
PFDA	11 ± 3.8	9 ± 1.9	< LOD	ng L^{-1}	1
PFUnA	4.5	3.3	< LOD	ng L^{-1}	2.5
PFDoA	< LOD	< LOD	< LOD	ng L^{-1}	2.5
PFTriDA	< LOD	< LOD	< LOD	ng L^{-1}	5.1
PFTreA	< LOD	< LOD	< LOD	ng L^{-1}	5.1
4:2 FTS	< LOD	26.7 ± 0.6	6 ± 1	ng L^{-1}	2.5
8:2FTS	34 ± 2.5	146.600 ± 0.004	< LOD	ng L^{-1}	5.1
NEtFOSAA	< LOD	< LOD	< LOD	ng L^{-1}	
PFPeS	90 ± 71	850 ± 52	120 ± 30	ng L^{-1}	1.0
PFHpS	13 ± 2.3	700 ± 130	75 ± 5	ng L^{-1}	1.0
PFNS	< LOD	50 ± 4.7	< LOD	ng L^{-1}	5.0
PFDS	< LOD	< LOD	< LOD	ng L^{-1}	5.1
FOSA	< LOD	70 ± 16	500 ± 110	ng L^{-1}	2.5
N-MeFOSA	< LOD	< LOD	< LOD	ng L^{-1}	2.4
NMeFOSAA	< LOD	< LOD	< LOD	ng L^{-1}	10.1
Total:	5400± 200	22100± 700	11000± 200	ng L^{-1}	

The effluent samples were normalized to the average measured concentrations for the pre-filtered groundwaters during infusion. The effluent samples reached the C_o concentration quickly (within ~2000 PV) relative to the synthetic groundwater, most likely due to the complexity of the PFAS mixture and the presence of native dissolved organic matter that could compete for adsorption sites. Assuming the average faster paced ground water could move around ~ .3048 m day^{-1} (1ft day^{-1}), 2000 PV translated to ~18 years for each m^3 of treated aquifer.

5.0 IMPLICATIONS FOR FUTURE RESEARCH AND BENEFITS

This one-year proof-of-concept study had the intent of bridging the gap between the polymer synthesis and PFAS adsorption studies conducted under SERDP project (ER18-1052, *Remediation of Per- and Polyfluoroalkyl Impacted Groundwater Using Cationic Hydrophobic Polymers as Ultra-High Affinity Sorbents,* PI Sierra-Alvarez) and assessment of in situ applications of polymer-based PFAS removal from impacted geomedia systems.

Research that could be addressed following 1-year proof-of-concept study: Based on the results of the current proof-of-concept study, several tasks could be pursued in a subsequent 2-year project:

- Flow-through column data fitting to the advection-dispersion equation with chemical retardation enabling direct quantitative comparison to distribution coefficients determined from the batch experiments conducted in the current work and field scale prediction.
- Further optimization of cPOT synthesis to increase effectiveness toward its non-colloidal counterpart, which would enable tailoring injection mixtures for site-specific conditions.
- Assessment of the long-term fate of the colloidal polymers in the subsurface, including their susceptibility to microbial biodegradation and potential generation of hazardous byproducts as amine based polymers.
- Mesocosm scale injection into a lab-built aquifer model to test larger-scale injection, mobility, and retention patterns of cPANI as well as PFAS remediation.
- Field scale efficacy testing in an impacted site by injecting the cPANI downstream of a PFAS plume.

6.0 LITERATURE CITATIONS AND PUBLISHED PRODUCTS

Liu, C., J. Hatton, W. A. Arnold, M. F. Simcik and K. D. Pennell (2020). "In situ sequestration of perfluoroalkyl substances using polymer-stabilized powdered activated carbon." *Environmental Science and Technology* 54(11): 6929-6936.

McGregor, R. (2018). "In situ treatment of PFAS-impacted groundwater using colloidal activated carbon." Remediation Journal 28: 33-41.

McGregor, R. (2020). "Six pilot-scale studies evaluating the in situ treatment of PFAS in groundwater." Remediation 30(3): 39-50.

Sierra-Alvarez, R., J. A. Field, J. Chorover, L. A. Abrell and Y. Olshansky (2019). "Remediation of per- and polyfluoroalkyl contaminated groundwater using cationic hydrophobic polymers as ultra-high affinity sorbents." *Interim Report, SERDP Project ER18-1052, July 2019*.

Simcik, M. F., W. A. Arnold and K. Pennell (2019). "Development of a novel approach for in situ remediation of PFC contaminated groundwater systems." Strategic Environmental Research and Development Program (SERDP) and Environmental Security Technology Certification Program (ESTCP), Alexandria, VA. March, 2019.

Tufenkji, N. and M. Elimelech (2004). "Correlation equation for predicting single-collector efficiency in physicochemical filtration in saturated porous media." Environmental Science and Technology 38(2): 529-536.